analytical chemistry

pubs.acs.org/ac Article

In Situ Observation of Glucose Metabolism Dynamics of Endothelial Cells in Hyperglycemia with a Stretchable Biosensor: Research Tool for Bridging Diabetes and Atherosclerosis

Meihong Peng, Xu Zhao, Chao Wang, Lihao Guan, Kai Li, Chaoyue Gu, and Yuqing Lin*

Cite This: https://dx.doi.org/10.1021/acs.analchem.0c03938 Read Online

ACCESS | Metrics & More | Article Recommendations | Supporting Information

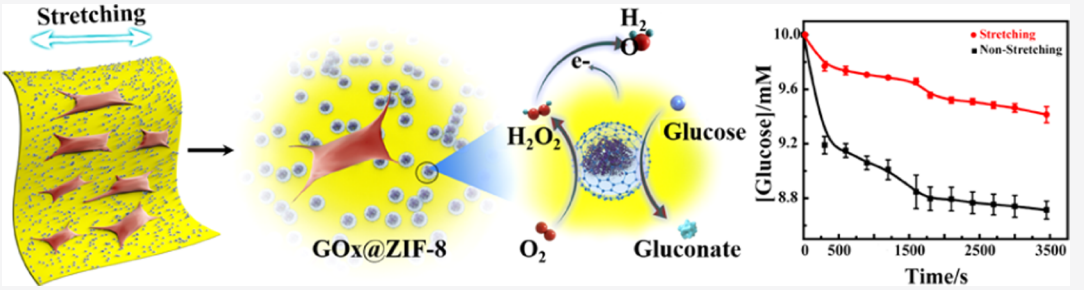

ABSTRACT: Diabetes is a metabolic syndrome associated with hyperglycemia, hypertension, atherosclerosis, and endothelial dysfunction. Applying the mechanical stretch on cells to simulate blood circulation while monitoring the cell glucose metabolism in a high-glucose environment is important for better comprehension of the underlying mechanisms of atherosclerosis caused by diabetes. Herein, we developed a facile strategy integrating zeolitic imidazolate framework-8-encapsulated glucose oxidase (GOx@ZIF-8) and an gold (Au) stretchable electrode (Au SE) to construct a flexible and stretchable glucose sensor (GOx@ZIF-8/Au SE) for investigating the glucose metabolism mechanism of stretched endothelial cells in hyperglycemia. The encapsulation of GOx with ZIF-8 prevents the aggregation and detachment of GOx from the sensing interface and endows the biosensor with high stability. Additionally, the Au SE with inherent stretchability can act as an integrated platform for mechanical stimulation as well as for transient signal sensing during the mechanotransduction process. Moreover, this flexible and stretchable glucose sensor is successfully used for monitoring the glucose metabolism of mechanically stimulated cells in hyperglycemia, and it was found for the first time that the glucose utilization ability of cells under static conditions is higher than that in the stretched state. This facile and straightforward method paves a promising route for designing a stable enzyme-based stretchable biosensor for detecting the underlying mechanisms of atherosclerosis caused by diabetes.

INTRODUCTION

Atherosclerosis is one of the main complications of diabetes involving multiple causative factors including dysfunction of the vascular endothelium.[1] Dysfunction of the vascular endothelium is a hallmark of most conditions that are associated with both diabetes and atherosclerosis.[1,2] Previous reports have proved that the hyperglycemia (a main property of diabetes) status can induce endothelial dysfunction.[3,4] Therefore, it is of great significance to investigate the pathology of atherosclerosis by monitoring the endothelial cell (EC) glucose metabolism in hyperglycemia. ECs are arranged on the walls of all blood vessels and exposed to the mechanical forces of blood flow. These mechanical forces modulate their function and play an important role in maintaining the homeostasis of circulation as well as regulating it in blood vessels.[5] Evidently, monitoring the cell glucose metabolism in a high-glucose environment while applying the mechanical stretch on cells to simulate blood circulation is important for better comprehension of the underlying mechanisms of atherosclerosis caused by diabetes. However, few reports currently involve tracking the glucose metabolism of ECs under mechanical stimulation.

Among various detection technologies, the electrochemical method with good sensitivity, high selectivity and excellent spatiotemporal resolution is widely used to monitor and quantify active substances, especially the instantaneous signal.[6] As glucose is an electrochemically inert substance, glucose oxidase (GOx) is always adopted to fabricate a glucose biosensor.[7−12] For instance, we have constructed online electrochemical systems for instantaneous and continuous

Received: September 17, 2020
Accepted: November 26, 2020

Scheme 1. Fabrication Process of GOx@ZIF-8/Au SE and the Mechanism of Cellular Glucose Metabolism Monitoring

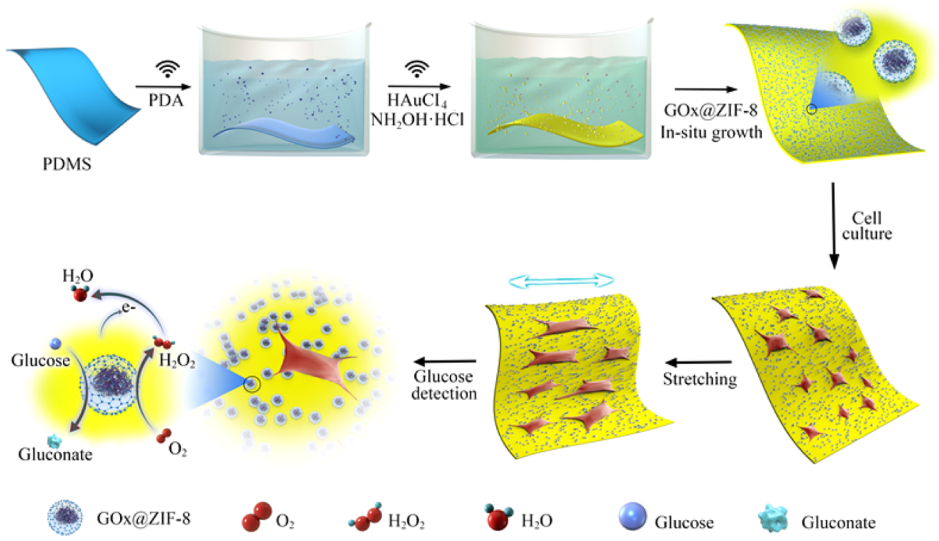

monitoring of glucose in the rat brain.[8,9] However, because of the intrinsic property of enzymes such as poor stability and being prone to aggregation, the enzyme-based sensors still have some inherent shortcomings including insufficient long-term stability and low sensitivity.[10−12] Therefore, the development of GOx-immobilization techniques with high efficiency is the crux for the stabilization of enzymes. Metal−organic frameworks (MOFs) are composed of metal ions and organic ligands,[13,14] and enzymes can tightly combine with MOFs through the interactions including hydrogen bonds, van der Waals forces, covalent and/or coordinative bonds.[15] Because of excellent biocompatibility and mild synthetic conditions, zeolitic imidazolate framework-8 (ZIF-8) has been widely reported to accommodate GOx and prevent the damage of GOx from external harsh conditions.[16−18]

The sensor constructed on a rigid electrode for a mechanotransduction-related study has two non-negligible disadvantages. On the one hand, the cell morphology always changed with the mechanical force, which can lead to constant changes in the distance between the rigid electroactive surface and the cell.[19] On the other hand, the mechanical stimulation platform and the sensor system are independent of each other, failing to in situ and real-time monitoring of instantaneous signals of cells. Therefore, it is crucial to establish an integrated platform for accurate and sensitive sensing of signals from cell mechanotransduction, accompanied by mechanical stimulation. In the last several years, the flexible and stretchable electrochemical sensor for inducing and monitoring cell mechanotransduction in real time catches the sight of scientists.[20−26] For instance, Huang group integrated carbon nanotubes, gold nanotubes, and titanium dioxide nanoparticles to construct a stretchable 5-hydroxytryptamine (5-HT) sensor with antifouling and decontamination properties, enabling the real-time monitoring of distension-evoked 5-HT release from the ileum.[25] We developed an environmentally friendly ultraviolet-irradiation-assisted technique to fabricate a stretchable, nanostructured Au film as a flexible electrode for the detection of nitric oxide released from mechanically sensitive cells.[22] Very recently, we first found that the nickel single-atom based electrocatalyst can facilitate NO oxidation and fabricated a flexible electrochemical sensor for the real-time NO sensing in a live cellular environment.[26] However, as far as we know, there is no report on the flexible and stretchable biosensors as an analytical method for real-time monitoring of glucose metabolism of cells under mechanical stimulation.[23,27−30]

In this study, we demonstrated a facile strategy to design a flexible and stretchable biosensor for continuous glucose metabolism monitoring of stretched cells in hyperglycemia. As schematically described in Scheme 1, the Au stretchable electrode (Au SE) fabricated by the ultraviolet irradiation method is immersed in the mixture of GOx and ZIF-8 precursor and in the process of ZIF-8 growth, GOx was encapsulated into the ZIF-8 and anchored on the surface of flexible Au SE directly by biomimetic mineralization to construct a GOx@ZIF-8/Au SE. Compared with the ZIF-8-free biosensor in which GOx was directly adsorbed on the Au SE (GOx/Au SE), GOx@ZIF-8/Au shows better stability and selectivity toward glucose sensing, benefiting from ZIF-8 preventing the aggregation and detachment of GOx and thus maintaining the high catalytic activity of GOx. This glucose sensor is successfully used for monitoring the glucose metabolism of mechanically stimulated human umbilical vein endothelial cells (HUVECs) under simulated hyperglycemia conditions, revealing the capability for investigating the underlying mechanism of atherosclerosis caused by diabetes.

EXPERIMENTAL SECTION

Fabrication of Flexible GOx@ZIF-8/Au SE. The polydimethylsiloxane (PDMS) membrane (~300 μm thick) was prepared by the spin-coating method according to the reported procedure.[22] The flexible Au film electrode was synthesized by an ultrasonic method. Briefly, the PDMS substrate was soaked in a 5 mg/mL dopamine (DA) solution (dissolved in 5 mM Tris, pH 8.5) to grow amino ($-NH_2$) and hydroxyl (−OH) functional groups on the surface, endowing the PDMS surface with a better affinity. The PDMS membrane was immersed in a mixed solution of chloroauric acid (3 mL, 5 mM) and hydroxylamine hydrochloride (2 mL, 40 mM). After 3 min of ultrasonication, a flexible Au film was formed by static incubation for 4 h.

3-Mercaptopropionic acid (MPA)-modified Au film electrode was prepared by immersing the freshly prepared Au film electrode in 1 mM MPA solution for 30 min and then the electrode was rinsed carefully with deionized water to remove

https://dx.doi.org/10.1021/acs.analchem.0c03938
Anal. Chem. XXXX, XXX, XXX−XXX

the nonchemisorbed MPA. A total of 0.4 g of 2-methylimidazole (108 mM) was dissolved in 10 mL of ultrapure Milli-Q water, and then 5 mg of GOx (817 units) was added to the above solution. This mixture was slightly yellow in color and labeled as A. A total of 0.02 g of $Zn(NO_3)_2{\cdot}6H_2O$ (1.53 mM) was dissolved in another 10 mL of ultrapure Milli-Q water separately and labeled as B. The MPA-modified Au film was immersed in the mixture of B and A with gentle shaking at room temperature for 3 h to obtain the flexible and stretchable GOx@ZIF-8/Au SE.

HUVEC Culture. HUVECs were routinely cultured in a culture medium (430167) with 84% high glucose-Dulbecco's modified eagle medium (H-DMEM), 15% fetal bovine serum, 1% penicillin, and streptomycin at 37 °C in a humidified incubator (95% air with 5% CO_2). The flexible electrodes were placed in a Petri dish and kept in the incubator for 24 h to allow cell adhesion. For cell detection, HUVECs were seeded on electrodes at a density of ~4.82×10^5 cell/cm^2.

RESULTS AND DISCUSSION

SEM and Element Characterization of GOx@ZIF-8/Au SE. First, physical characterization techniques were applied to characterize the morphology and structure of synthesized ZIF-8, GOx@ZIF-8, Au SE, and GOx@ZIF-8/Au SE. Figure 1A shows a uniform hydrangea structure with smooth surfaces. The petals of hydrangea with an average thickness of 280 nm are exhibited in the Au film SE. The scanning electron microscopy (SEM) images in Figure S1 proved that ZIF-8 of a typical dodecahedron structure was successfully synthesized with an average size of 800 nm. The SEM image of GOx@ZIF-8 (Figure 1B) displays that the morphology and size of most ZIF-8 have a huge difference before and after GOx encapsulation, which should result from the interaction between ZIF-8 and GOx. Compared with the pristine nanostructured Au film SE, the surface of the GOx@ZIF-8/Au SE becomes rougher and the average thickness of the petal increases to 540 nm. Obviously, the surface structure of Au nanoflowers is similar to that of synthesized GOx@ZIF-8, demonstrating that GOx@ZIF-8 was successfully anchored on the Au SE (Figure 1C). X-ray diffraction (XRD) and energy-dispersive X-ray spectroscopy (EDX) were performed to further characterize the chemical structure of the fabricated materials. As shown in Figure S2, the ZIF-8/Au film has typical peaks corresponding to the (111), (200), (220), and (311) crystal planes of Au, and the synthesized ZIF-8 and ZIF-8/Au film have a series of diffraction peaks similar to the simulated peaks of pure ZIF-8.[27,28] The peaks in the EDX spectra of GOx@ZIF-8/Au SE (Figure 1D) corresponded to C, N, Au, Si, and Zn elements. These results confirm that ZIF-8 was successfully synthesized on the surface of Au film.

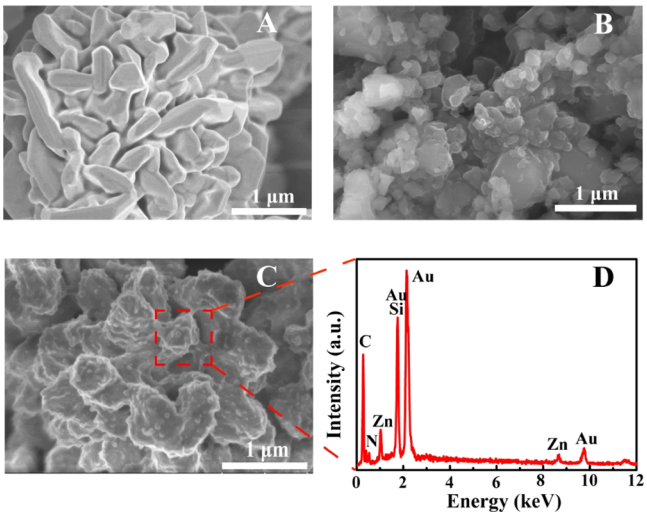

Figure 1. SEM images of (A) Au film SE, (B) GOx@ZIF-8, and (C) GOx@ZIF-8/Au SE. (D) EDX spectra of GOx@ZIF-8/Au SE.

Electrochemical Characterization and Flexibility Test of GOx@ZIF-8/Au SE. Before GOx@ZIF-8 was anchored, the Au film SE (0.5 cm in length and 0.5 cm in width) was activated by scanning cyclic voltammetry (CV) in 0.5 M H_2SO_4 (Figure S3A). Based on the charge of the typical reduction peak of Au oxide at around 0.9 V being 2.207×10^{-4} C, an entire active area of such Au film SE was calculated to be 0.572 cm^2,[29] which was approximately 2-fold that of the geometry area, indicating that the electrode surface consists of gold nanoparticles and that the surface is relatively coarse. Furthermore, no discernible alterations in the CV curves of Au film SE are observed during 50 cycles after stretched different times at different degrees and bent at different curvatures (Figure S3), demonstrating the electrochemical stability of the Au film against large mechanical bending and stretching. The SEM images of Au film SE in Figure S4 prove that the larger reaction surface area and the high electrochemical stability of the electrode can be mainly attributed to the Au nanostructure of the Au film. Therefore, the Au film retains good electrochemical stability in the deformed state, demonstrating that the Au film can be used as a flexible conductive substrate for growing GOx@ZIF-8.[30,31]

Electrochemical behavior of the GOx@ZIF-8/Au SE has been studied in $FcCH_2OH$ solution after being subjected to harsh conditions, including stretching to different tensile strains and times and bending into different curvatures 10 times as well as to a radius of 0.50 cm different times. Figure 2 exhibits that the peak current and potential of ferricyanide have high repeatability, indicating that the GOx@ZIF-8/Au SE has significant antimechanical bending and stretching ability.

Electrochemical Response and Amperometric Sensing of Glucose on GOx@ZIF-8/Au SE. To investigate the sensing performance of GOx@ZIF-8/Au SE for glucose, CV of GOx@ZIF-8/Au SE was performed in a phosphate-buffered saline (PBS) solution and PBS-containing different concentrations of glucose. The results in Figure 3A,B show that the reduction current starts to increase significantly at −0.3 V because the hydrogen peroxide produced from glucose oxidation was reduced, and the reduction current gradually increased as the glucose concentration increased, demonstrating that GOx@ZIF-8/Au SE had significant response to glucose.

To verify the capability of glucose monitoring with the GOx@ZIF-8/Au SE, linearity and selectivity experiments were performed in PBS (pH 7.4). The reduction current of GOx@ZIF-8/Au SE shows increasing stepwise responses with the addition of different concentrations of glucose (Figure 3B,C). As the inset image in Figure 3C shows, the GOx@ZIF-8/Au SE exhibited excellent detection linearity toward different concentrations of glucose. The linear regions of glucose concentration are from 0.02 to 1.41 mM, and the detection limit is calculated to be 1.8 μM (S/N = 3), according to the formula: I (μA) = −2.89C (mM) − 0.74. Those potential interference analytes including DA, uric acid (UA), ascorbic

https://dx.doi.org/10.1021/acs.analchem.0c03938
Anal. Chem. XXXX, XXX, XXX−XXX

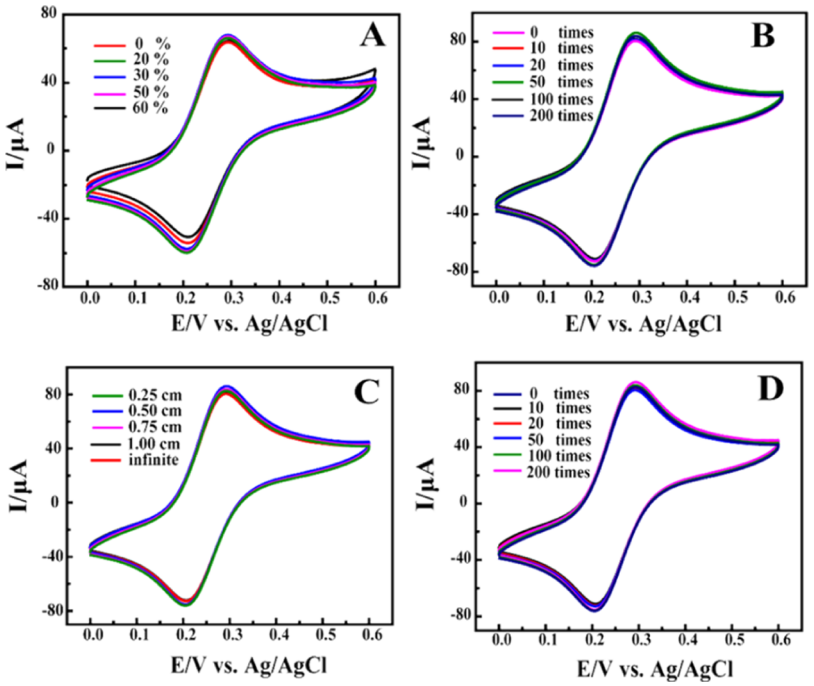

Figure 2. CV responses of the GOx@ZIF-8/Au SE in 1 mM $FcCH_2OH$ solution with the electrode (A) stretched to different tensile strains, (B) stretched different times (stretched by 20%), (C) bent to different curvatures 10 times, and (D) bent different times with a bending radius of 0.5 cm.

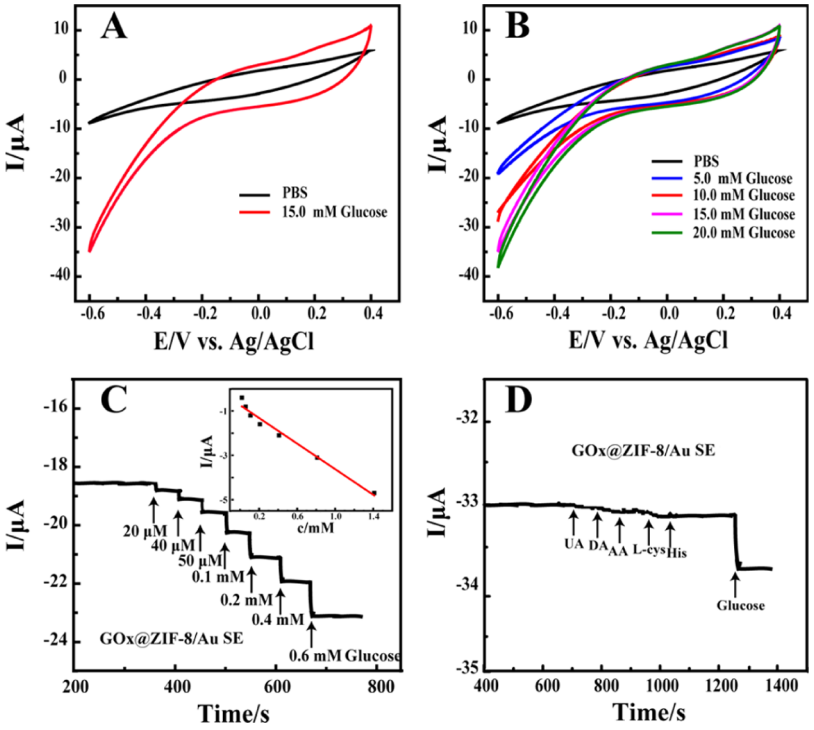

Figure 3. Electrochemical performance of GOx@ZIF-8/Au SE. (A) CV curves in the presence and absence of 16 mM glucose. (B) CV curves in the presence of different concentrations of glucose. (C) Chronoamperometry curves with different concentrations of glucose (inset: linear relationship between the current change and glucose concentration). (D) Chronoamperometry curve after the addition of 90 μM glucose and interfering substances: UA 50 μM; DA 20 μM; AA 50 μM; L-cys 20 μM; and His 20 μM. (The conducting potential is −0.3 V vs Ag/AgCl.)

acid (AA), L-cystine (L-cys), and histidine (His) were studied for selectivity experiments.[32] The result depicted in Figure 3D demonstrates that the synthesized GOx@ZIF-8/Au SE has excellent anti-interference ability because of the low interference response to detect 90 μM glucose in the biological environment. The above data indicate that the enzyme encapsulated in ZIF-8 still has good catalytic activity and specificity for glucose oxidation.

For further exploring the working mechanism of the biosensor, chronoamperometry experiments were conducted

https://dx.doi.org/10.1021/acs.analchem.0c03938
Anal. Chem. XXXX, XXX, XXX−XXX

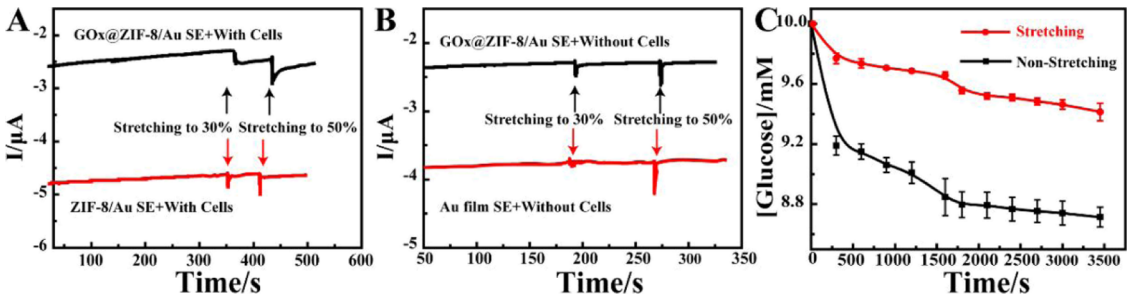

Figure 4. (A) Electrochemical response of the cell cultured on GOx@ZIF-8/Au SE and ZIF-8/Au SE with different degrees of stretching. (B) Electrochemical response of the GOx@ZIF-8/Au SE and the Au film SE at different degrees of stretching. (C) Real-time monitoring of glucose uptake of stretched or static cells by GOx@ZIF-8/Au SE. The conducting potential is −0.3 V, as opposed to Ag/AgCl.

to study the response of GOx/Au SE and Au film SE to H_2O_2 or glucose. Figure S5A shows that as a series of different concentrations of H_2O_2 were injected (from 0.5 to 8 mM), the degree of drop in the reduction current increased gradually, indicating that the flexible Au film electrode can detect the signal of H_2O_2. Figure S5B shows that the reduction currents of the flexible Au film SE and the GOx/Au SE did not change significantly when different concentrations of glucose were continuously injected and the electrochemical performance of GOx/Au SE is not stable during the experiment. The responses of GOx/Au SE and GOx@ZIF-8/Au SE to glucose show that the GOx@ZIF-8/Au SE has higher stability and sensitivity toward glucose sensing. It can be explained by the following reasons: as the force between the GOx and the Au film is not strong enough, when the sensor was exposed to the solution, the GOx loaded on the GOx/Au SE surface tends to leave, causing the amount of GOx anchored on the Au film to decrease. Additionally, enzymes directly fabricated on the surface of Au SE are prone to aggregation in the test solution, resulting in reduced catalytic activity.[33] For the GOx@ZIF-8/Au SE, GOx@ZIF-8 is stably anchored on the surface of Au film SE, and the GOx which is protected by ZIF-8 still has good catalytic activity and specificity toward glucose oxidation.[33,34] The above results further confirm that the GOx@ZIF-8/Au SE can be used to effectively detect glucose in the biological environment.

Monitoring the Glucose Metabolism of HUVECs Using GOx@ZIF-8/Au SE. As an integrated platform of glucose sensing and mechanical inducing, the GOx@ZIF-8/Au SE allows for in situ and real-time monitoring of cell glucose metabolism during the mechanotransduction process. Before the experiment, the state of living cells was observed first. As shown in Figure S6, compared with the cells cultured for 24 h, the number of cells cultured for 72 h was greatly increased, and the HUVECs were spindle-shaped and arranged neatly in a clean Petri dish, proving that the cells were in good condition.[31] The cells were cultured on GOx@ZIF-8/Au SE and ZIF-8/Au SE in the Petri dish for 24 h for the next experiment. To demonstrate that the change in the current involves the glucose metabolism of stimulated cells, two group of control experiments were conducted. In Figure 4A, only a weak current signal was presented on the GOx-free electrode after mechanical stimulation, in which the current change is probably caused by the H_2O_2 released from the mechanically stimulated cells.[35] As a comparison, a much significant response on the GOx@ZIF-8/Au SE under the same condition was observed, confirming the current response of the GOx@ZIF-8/Au SE indeed originated from the release of glucose, and the glucose released from the cell during the 30 and 50% stretched states was approximately 0.080 and 0.093 mM, respectively. There are two types of glucose transporters in cell membranes: sodium-dependent glucose transporters (SGLTs) for active glucose transport and glucose transporters (GLUT) that transport glucose along a concentration gradient.[36] Previous reports have shown that mechanical force can change the conformation of GLUT in the cell membrane and increase the transport rate along the concentration gradient,[37] which can reasonably explain the glucose release upon cell stretching in Figure 4A. In addition, the same mechanical stimulation to GOx@ZIF-8/Au SE and ZIF-8/Au SE without cells generated no perceptible current response (Figure 4B), further indicating that the increase of the reduction current is caused by glucose released from mechanically stimulated cells. These results substantially demonstrate that the GOx@ZIF-8/Au SE could sensitively monitor the glucose metabolism in the cellular environment.

As an interface between the blood flow and the vessel wall, ECs are mechanically stimulated by shear stress of the blood flow and the circumferential stress from the blood pressure.[5] Those biochemical molecules released from the ECs−blood flow interaction are important determinants of vascular homeostasis.[25] Glucose metabolism is not only the main source of energy for cells but also associated with a lot of diseases, such as Alzheimer's disease and diabetic angiocardiopathy.[38,39] Atherosclerosis is one of the main complications of diabetes involving multiple causative factors including the dysfunction of the vascular endothelium.[1] Considering that the hyperglycemia status can induce endothelial dysfunction,[4] we use GOx@ZIF-8/Au SE to continuously record HUVEC glucose metabolism in the hyperglycemia status for exploring the underlying mechanism of atherosclerosis caused by diabetes. In this experiment, the cells were mechanically stimulated by stretching GOx@ZIF-8/Au SE to simulate the mechanical force on cells from blood circulation. Figure 4C shows that the original 10 mM glucose (hyperglycemia is defined as a blood glucose concentration over 7.8 mM) in the cell culture system gradually decreased, either in the stretched (red curve) or static state (black curve), revealing that the glucose has been uptaken by cells cultured on the GOx@ZIF-8/Au SE surface. The glucose utilization rate of cells under mechanical stimulation is calculated to be 2.2 fM min^{-1} $cell^{-1}$, while the rate of glucose assimilated by cells in the static state is 6.6 fM min^{-1} $cell^{-1}$, which is similar to the previously reported value (8.8 fM min^{-1} $cell^{-1}$).[40] By comparing the glucose utilization degree, it is found that the ability of cells to utilize glucose under static conditions is higher than that under

https://dx.doi.org/10.1021/acs.analchem.0c03938
Anal. Chem. XXXX, XXX, XXX−XXX

stretched conditions in a high-glucose environment. Studies have shown that SGLT is widely expressed in HUVECs, and the high glucose environment can stimulate cells to synthesize SGLT1 protein for glucose transport from the exocellular environment.[41] However, protein kinase C produced in the process of stretching can highly and negatively affect the activity of SGLT.[42,43] These may explain that the glucose consumption ability of cells under static conditions is higher than that in the stretched state in Figure 4C.

According to the literature, hyperglycemia culture can increase the permeability of vascular ECs, leading to the increase of basal membrane fibroblast growth factor-2, which promotes the apoptosis of arterial ECs induced by tumor necrosis factor-α.[44,45] Moreover, diabetes activates the expression of ECs and cellular adhesion molecules by increasing the release of cytokines, mediating platelet activation and adhesion to activated ECs, leading to vascular occlusion.[46,47] Combined with our experimental results, it is reasonable to speculate that the hyperglycemia condition will impede the blood flow by activating platelet adhesion on ECs, thus slowing down the blood flow, reducing the stretching degree of ECs leading to an increase in cellular glucose intake, and further leading to atherosclerosis.

CONCLUSIONS

In summary, we successfully developed a feasible and efficient method for anchoring GOx@ZIF-8 on the Au film surface, constructing a stretchable and flexible GOx@ZIF-8/Au SE for in situ and real-time glucose monitoring. The inherent stretchability allows this sensor to act as an integrated platform for mechanical stimulation and sensing transient signals during the mechanotransduction process. The encapsulation of GOx with ZIF-8 prevents the aggregation and detachment of GOx from the sensing interface and endows the biosensor with high stability. This sensor was successfully used for monitoring the glucose metabolism of mechanically stimulated cells under simulated hyperglycemia conditions, demonstrating the potential capability for detecting the underlying mechanisms of atherosclerosis caused by diabetes. In addition, this simple and straightforward method paves the way for designing a stretchable and flexible biosensor and exhibits the potential capability for investigating the underlying mechanisms of physiological and pathological processes related to mechanotransduction.

ASSOCIATED CONTENT

Supporting Information

The Supporting Information is available free of charge at https://pubs.acs.org/doi/10.1021/acs.analchem.0c03938.

Chemicals, instrumentation, SEM image of ZIF-8, XRD patterns of ZIF-8/Au film, ZIF-8, and simulated ZIF-8, voltammetric responses of the Au film SE in 0.5 M H_2SO_4, voltammetric responses of the Au film SE in 1 mM $FcCH_2OH$ solution with the film exposed to different mechanical forces, SEM images of the Au film SE before stretching and under stretching, amperometric response of the Au film SE with sequent addition of H_2O_2, amperometric response of the GOx/Au SE and Au film SE with sequent addition of glucose, and microscopy image of HUVECs (PDF)

AUTHOR INFORMATION

Corresponding Author

Yuqing Lin − *Department of Chemistry, Capital Normal University, Beijing 100048, China;* orcid.org/0000-0003-1501-5005; Phone: +86 1068903047; Email: linyuqing@cnu.edu.cn; Fax: +86 1068903047

Authors

Meihong Peng − *Department of Chemistry, Capital Normal University, Beijing 100048, China*

Xu Zhao − *Department of Chemistry, Capital Normal University, Beijing 100048, China*

Chao Wang − *Department of Chemistry, Capital Normal University, Beijing 100048, China*

Lihao Guan − *Department of Chemistry, Capital Normal University, Beijing 100048, China*

Kai Li − *Department of Chemistry, Capital Normal University, Beijing 100048, China*

Chaoyue Gu − *Department of Chemistry, Capital Normal University, Beijing 100048, China*

Complete contact information is available at: https://pubs.acs.org/10.1021/acs.analchem.0c03938

Author Contributions

M.P. and X.Z. contributed equally to this work. The manuscript was written through contributions of all authors. All authors have given approval to the final version of the manuscript.

Notes

The authors declare no competing financial interest.

ACKNOWLEDGMENTS

This work was financially supported by National Natural Science Foundation (22074095), High-Level Teachers in Beijing Municipal Universities in the Period of 13th Five-Year Plan (CIT&TCD20190330), Scientific Research Project of Beijing Educational Committee (KM201810028008), and Youth Innovative Research Team of Capital Normal University.

REFERENCES

(1) Sala, L. L.; Prattichizzo, F.; Ceriello, A. *Eur. J. Prev. Cardiol.* **2019**, *26*, 15−24.

(2) Lewis, J.; Kottke, B. *Science* **1977**, *196*, 1007−1009.

(3) Schiano, C.; Grimaldi, V.; Franzese, M.; Fiorito, C.; De Nigris, F.; Donatelli, F.; Soricelli, A.; Salvatore, M.; Napoli, C. *Toxicol. In Vitro* **2020**, *62*, 104694.

(4) Ceriello, A.; Taboga, C.; Tonutti, L.; Quagliaro, L.; Piconi, L.; Bais, B.; Da Ros, R.; Motz, E. *Circulation* **2002**, *106*, 1211−1218.

(5) Tarbell, J. M.; Pahakis, M. Y. *J. Intern. Med.* **2006**, *259*, 339−350.

(6) Xiao, T.; Wu, F.; Hao, J.; Zhang, M.; Yu, P.; Mao, L. *Anal. Chem.* **2017**, *89*, 300−313.

(7) Xu, C.; Wu, F.; Yu, P.; Mao, L. *ACS Sens.* **2019**, *4*, 3102−3118.

(8) Lin, Y.; Liu, K.; Yu, P.; Xiang, L.; Li, X.; Mao, L. *Anal. Chem.* **2007**, *79*, 9577−9583.

(9) Lin, Y.; Zhu, N.; Yu, P.; Su, L.; Mao, L. *Anal. Chem.* **2009**, *81*, 2067−2074.

(10) DiCosimo, R.; McAuliffe, J.; Poulose, A. J.; Bohlmann, G. *Chem. Soc. Rev.* **2013**, *42*, 6437−6474.

(11) Jin, Z.; Han, S.-Y.; Zhang, L.; Zheng, S.-P.; Wang, Y.; Lin, Y. *Bioresour. Technol.* **2013**, *130*, 102−109.

(12) Tang, J.; Wang, Y.; Li, J.; Da, P.; Geng, J.; Zheng, G. *J. Mater. Chem. A* **2014**, *2*, 6153−6157.

(13) Van Vleet, M. J.; Weng, T.; Li, X.; Schmidt, J. *Chem. Rev.* **2018**, *118*, 3681−3721.
(14) Yang, Q.; Xu, Q.; Yu, S.-H.; Jiang, H.-L. *Angew. Chem., Int. Ed.* **2016**, *55*, 3685−3689.
(15) Majewski, M. B.; Howarth, A. J.; Li, P.; Wasielewski, M. R.; Hupp, J. T.; Farha, O. K. *CrystEngComm* **2017**, *19*, 4082−4091.
(16) Maleki, A.; Shahbazi, A. A.; Alinezhad, V.; Santos, H. A. *Adv. Healthcare Mater.* **2020**, *9*, 2000248.
(17) Cheng, K.; Svec, F.; Lv, Y.; Tan, T. *Small* **2019**, *15*, 1902927.
(18) Hu, Y.; Liao, J.; Wang, D.; Li, G. *Anal. Chem.* **2014**, *86*, 3955−3963.
(19) Schulte, A.; Schuhmann, W. *Angew. Chem., Int. Ed.* **2007**, *46*, 8760−8777.
(20) Xu, K.; Lu, Y.; Takei, K. *Adv. Mater. Technol.* **2019**, *4*, 1800628.
(21) Liu, Y.-L.; Qin, Y.; Jin, Z.-H.; Hu, X.-B.; Chen, M.-M.; Liu, R.; Amatore, C.; Huang, W.-H. *Angew. Chem., Int. Ed.* **2017**, *56*, 9454−9458.
(22) Zhao, X.; Wang, K.; Li, B.; Wang, C.; Ding, Y.; Li, C.; Mao, L.; Lin, Y. *Anal. Chem.* **2018**, *90*, 7158−7163.
(23) Liu, Y.-L.; Huang, W.-H. *Angew. Chem., Int. Ed.* **2020**, *59*, 2−13.
(24) Jin, Z. H.; Liu, Y. L.; Fan, W. T.; Huang, W. H. *Small* **2020**, *16*, 1903204.
(25) Liu, Y. L.; Chen, Y.; Fan, W. T.; Cao, P.; Yan, J.; Zhao, X. Z.; Dong, W. G.; Huang, W. H. *Angew. Chem., Int. Ed.* **2020**, *59*, 4075−4081.
(26) Zhou, M.; Jiang, Y.; Wang, G.; Wu, W.; Chen, W.; Yu, P.; Lin, Y.; Mao, J.; Mao, L. *Nat. Commun.* **2020**, *11*, 3188.
(27) Bandodkar, A. J.; Jia, W.; Yardımcı, C.; Wang, X.; Ramirez, J.; Wang, J. *Anal. Chem.* **2015**, *87*, 394−398.
(28) Ferri, S.; Kojima, K.; Sode, K. *J. Diabetes Sci. Technol.* **2011**, *5*, 1068−1076.
(29) Trasatti, S.; Petrii, O. A. *Pure Appl. Chem.* **1991**, *63*, 711−734.
(30) Lacour, S. P.; Wagner, S.; Huang, Z.; Suo, Z. *Appl. Phys. Lett.* **2003**, *82*, 2404−2406.
(31) Lacour, S. P.; Chan, D.; Wagner, S.; Li, T.; Suo, Z. *Appl. Phys. Lett.* **2006**, *88*, 204103.
(32) Liu, Y.-L.; Jin, Z.-H.; Liu, Y.-H.; Hu, X.-B.; Qin, Y.; Xu, J.-Q.; Fan, C.-F.; Huang, W.-H. *Angew. Chem., Int. Ed.* **2016**, *55*, 4537−4541.
(33) Liang, K.; Coghlan, C.; Bell, S.; Doonan, C.; Falcaro, P. *Chem. Commun.* **2016**, *52*, 473−476.
(34) Liang, K.; Ricco, R.; Doherty, C.; Styles, M.; Bell, S.; Kirby, N.; Mudie, S.; Haylock, D.; Hill, A.; Doonan, C.; Falcaro, P. *Nat. Commun.* **2015**, *6*, 7240.
(35) Waters, C. M. *Am. J. Physiol.: Lung Cell. Mol. Physiol.* **2004**, *287*, L484−L485.
(36) Wright, E. M.; Loo, D. D. F.; Hirayama, B. A. *Physiol. Rev.* **2011**, *91*, 733−794.
(37) Li, Y.; Sun, C.; Zhang, Z.; Xu, S. *Biophys. Rep.* **1997**, *13*, 51−54.
(38) Butterfield, D. A.; Halliwell, B. *Nat. Rev. Neurosci.* **2019**, *20*, 148−160.
(39) Sasso, F. C.; Carbonara, O.; Nasti, R.; Raffaele, C.; Michele, M.; Giannantonio, T.; Roberto, N.; Cozzolino, T. *J. Am. Med. Assoc.* **2004**, *291*, 1857−1863.
(40) Qi, M.; Zhang, Y.; Cao, C.; Lu, Y.; Liu, G. *RSC Adv.* **2016**, *6*, 39180−39187.
(41) Meng, L.; Uzui, H.; Guo, H.; Tada, H. *Mol. Med. Rep.* **2018**, *17*, 6887−6892.
(42) Konishi, H.; Tanaka, M.; Takemura, Y.; Matsuzaki, H.; Ono, Y.; Kikkawa, U.; Nishizuka, Y. *Proc. Natl. Acad. Sci. U.S.A.* **1997**, *94*, 11233−11237.
(43) Wright, E.; Hirsch, J.; Loo, D.; Zampighi, G. *J. Exp. Biol.* **1997**, *200*, 287−293.
(44) Morss, A. S.; Edelman, E. R. *J. Biol. Chem.* **2007**, *282*, 14635−14644.
(45) Clyne, A. M.; Zhu, H.; Edelman, E. R. *J. Cell. Physiol.* **2008**, *217*, 86−92.
(46) Gaiz, A.; Mosawy, S.; Colson, N.; Singh, I. *Biomed. Pharmacother.* **2017**, *94*, 679−686.
(47) Kaur, R.; Kaur, M.; Singh, J. *Cardiovasc. Diabetol.* **2018**, *17*, 121.

https://dx.doi.org/10.1021/acs.analchem.0c03938
Anal. Chem. XXXX, XXX, XXX−XXX